Atmospheric Environment 44 (2010) 4553–4564

Contents lists available at ScienceDirect

Atmospheric Environment

journal homepage: www.elsevier.com/locate/atmosenv

# Pollution influences on atmospheric composition and chemistry at high northern latitudes: Boreal and California forest fire emissions

H.B. Singh [a,*], B.E. Anderson [b], W.H. Brune [c], C. Cai [d], R.C. Cohen [e], J.H. Crawford [b], M.J. Cubison [j], E.P. Czech [a], L. Emmons [f], H.E. Fuelberg [g], G. Huey [h], D.J. Jacob [i], J.L. Jimenez [j], A. Kaduwela [d], Y. Kondo [k], J. Mao [i], J.R. Olson [b], G.W. Sachse [b], S.A. Vay [b], A. Weinheimer [f], P.O. Wennberg [l], A. Wisthaler [m], the ARCTAS Science Team

[a] *NASA Ames Research Center, Moffett Field, CA 94035, USA*
[b] *NASA Langley Research Center, Hampton, VA, USA*
[c] *Pennsylvania State University, University Park, PA, USA*
[d] *California Environmental Protection Agency, Sacramento, CA, USA*
[e] *University of California, Berkeley, CA, USA*
[f] *National Center for Atmospheric Research, Boulder, CO, USA*
[g] *Florida State University, Tallahassee, FL, USA*
[h] *Georgia Institute of Technology, Atlanta, GA, USA*
[i] *Harvard University, Cambridge, MA, USA*
[j] *University of Colorado, Boulder, CO, USA*
[k] *University of Tokyo, Tokyo, Japan*
[l] *California Institute of Technology, Pasadena, CA, USA*
[m] *University of Innsbruck, Innsbruck, Austria*

ARTICLE INFO

*Article history:*
Received 12 April 2010
Received in revised form
5 August 2010
Accepted 11 August 2010

*Keywords:*
Arctic pollution
Ozone
Aerosols
Greenhouse gases
Wild fires
Models

ABSTRACT

We analyze detailed atmospheric gas/aerosol composition data acquired during the 2008 NASA ARCTAS (Arctic Research of the Composition of the Troposphere from Aircraft and Satellites) airborne campaign performed at high northern latitudes in spring (ARCTAS-A) and summer (ARCTAS-B) and in California in summer (ARCTAS-CARB). Biomass burning influences were widespread throughout the ARCTAS campaign. MODIS data from 2000 to 2009 indicated that 2008 had the second largest fire counts over Siberia and a more normal Canadian boreal forest fire season. Near surface arctic air in spring contained strong anthropogenic signatures indicated by high sulfate. In both spring and summer most of the pollution plumes transported to the Arctic region were from Europe and Asia and were present in the mid to upper troposphere and contained a mix of forest fire and urban influences. The gas/aerosol composition of the high latitude troposphere was strongly perturbed at all altitudes in both spring and summer. The reactive nitrogen budget was balanced with PAN as the dominant component. Mean ozone concentrations in the high latitude troposphere were only minimally perturbed ($<5$ ppb), although many individual pollution plumes sampled in the mid to upper troposphere, and mixed with urban influences, contained elevated ozone ($\Delta O_3/\Delta CO = 0.11 \pm 0.09$ v/v). Emission and optical characteristics of boreal and California wild fires were quantified and found to be broadly comparable. Greenhouse gas emission estimates derived from ARCTAS-CARB data for the South Coast Air Basin of California show good agreement with state inventories for $CO_2$ and $N_2O$ but indicate substantially larger emissions of $CH_4$. Simulations by multiple models of transport and chemistry were found to be broadly consistent with observations with a tendency towards under prediction at high latitudes.

Published by Elsevier Ltd.

## 1. Introduction

The Arctic is one of the most environmentally sensitive regions of the earth system. The warming in this part of the atmosphere is the largest with visible evidence seen in receding sea ice cover (IPCC, 2007). Surface observations have shown that the Arctic is

---

* Corresponding author.
*E-mail address:* hanwant.b.singh@nasa.gov (H.B. Singh).

1352-2310/$ – see front matter Published by Elsevier Ltd.
doi:10.1016/j.atmosenv.2010.08.026

affected by transported Eurasian pollution in winter–spring leading to phenomena such as "Arctic haze" (Rahn, 1981; Barrie, 1986; Shaw, 1995; Quinn et al., 2007, 2008). In the summer, gas and aerosol emissions from boreal forest fires in Siberia, Canada, and Alaska represent a major chemical and radiative perturbation to the Arctic atmosphere (Stocks et al., 1998; Soja et al., 2007; Shindell et al., 2007; Stone et al., 2008). Black carbon (soot, BC) in Arctic snow can change snow albedo, altering radiative balance in the region (Clarke and Noone, 1985; Hansen and Nazarenko, 2004; Preston and Schmidt, 2006; Flanner et al., 2007). Emissions from boreal fires can be transported long distances influencing air quality in various regions of the Northern Hemisphere and be injected in the stratosphere under special convective conditions (Fromm and Servranckx, 2003; Colarco et al., 2004; Morris et al., 2006; Leung et al., 2007; Real et al., 2007). Recent investigations have suggested that pollution influences in the Arctic are a year round multi-altitude phenomenon that are poorly simulated by models (Klonecki et al., 2003; Stohl, 2006; Law and Stohl, 2007; Shindell et al., 2008).

Within the framework of the 2007–2009 International Polar Year activities (http://www.ipy.org), a number of field campaigns were carried out as part of the POLARCAT (POLar study using Aircraft, Remote sensing, surface measurements and modeling of Climate, chemistry, Aerosols and Transport) program (http://www.polarcat.no/) to better understand the impact of transported and locally generated pollution on the composition, chemistry and climate of the Arctic atmosphere. In collaboration with POLARCAT partners, NASA carried out the ARCTAS (http://cloud1.arc.nasa.gov/arctas/) field campaign in the spring and summer of 2008 utilizing instrumented aircraft for detailed observations of the chemical and radiative properties of gases and aerosols in the Arctic and over California. Although high latitudes were the main focus in ARCTAS, collaboration with California Air Resources Board (CARB) offered a unique opportunity to compare mid-latitude and boreal forest fire emissions as well as provide unique information to test the quality of emission inventories and models in use in California. An overview of the design and implementation of the 2008 ARCTAS campaign and prevailing meteorological conditions has been provided by Jacob et al. (2010) and Fuelberg et al. (2010), respectively.

In this study we use statistical analysis, tracer observations, and models to analyze and interpret ARCTAS data collected largely by the NASA DC-8 (12 km ceiling). We compare the characteristics of boreal and California fire emissions and evaluate the impact of these and anthropogenic sources on atmospheric composition especially as it relates to ozone formation in the troposphere.

## 2. Deployments, flights, and measurements

The NASA DC-8 was based in Palmdale, California (35N, 118W) where all instrument integration and test flights were carried out. The spring deployment (ARCTAS-A) took place from April 1 to 21, 2008 from a base in Fairbanks, Alaska (65N, 148W) and involved nine DC-8 flights (75 flight hours) over the Arctic spanning the region from Alaska to Greenland. The first part of the summer deployment (June 17–24, 2008) was focused on California (ARCTAS-CARB) air quality where the DC-8 performed four flights (33 flight hours) from its base in Palmdale. From June 26 to July 14 (ARCTAS-B), the aircraft operated from a base in Cold Lake, Canada (54N, 110W) performing nine flights (75 flight hours) including a two-night stay in Thule to over-fly Summit, Greenland (73N, 39W). Additional data over California were collected during transit flights between Palmdale and Cold Lake.

The DC-8 was equipped to make highly sensitive high-frequency (1–10 s) in situ measurements of important greenhouse gases ($CO_2$, $CH_4$, $N_2O$), $O_3$ and key precursors ($NO_y$, $HO_x$, PAN, HCHO), OVOC (such as $CH_3COCH_3$, $CH_3OH$, $CH_3CHO$), aerosol composition ($SO_4^{--}$, $NO_3^-$, $NH_4^+$, organic aerosol-OA, black carbon-BC), aerosol physical and optical properties (number, size, volatility, microphysics, CCN, absorption, scattering), and key tracers ($CH_3CN$, HCN, CO, $SO_2$, $H_2O$). Complementing these were an array of slower in situ measurements of NMHC, OVOC, halocarbons, alkyl nitrates, and bulk aerosol. A UV-Lidar performed remote measurement of ozone and aerosol several kilometers above and below the aircraft. Additional details involving airborne instrumentation, flight planning process, and flight tracks are provided in Jacob et al. (2010).

## 3. Results & discussion

To relate the multiplicity of measurements performed on the DC-8, merged files using 10 s and 60 s time windows were created. In much of the analysis that follows, the 10 s merge has been used with only occasional reliance on the 60 s merge. For some species (e.g. OVOC, NMHC, $NO_2$, $SO_4^{--}$, $HNO_3$), duplicate measurements using different methods were available. In such instances we have preferred data obtained with more specific and fast response techniques. As an example, $HNO_3$ was measured by both a fast response CIMS (Chemical Ionization Mass Spectroscopy) technique and a slower mist chamber technique. Further analysis indicated that the mist chamber technique likely suffered from nitrate interference and we have preferred the CIMS $HNO_3$ data. AMS (Aerosol Mass Spectrometer) aerosol data (OA and $SO_4^{--}$) and PTR-MS (Proton Transfer Reaction Mass Spectrometer) gas phase data (OVOC and $CH_3CN$) have been used in preference to other slower chromatographic measurements. For $NO_x$ ($NO + NO_2$) we have largely used the chemiluminescence data that are broadly in agreement with the LIF (Laser Induced Fluorescence) $NO_2$ data. An unknown fraction of $CH_3OONO_2$, present mostly in the upper troposphere, may have appeared as an artifact in $NO_x$ measurements and its upper limit has been estimated using a steady state model. In most other instances fast response data for $O_3$ and $NO_y$ (Chemiluminescence), $CO–CH_4–N_2O$ (Tunable diode laser spectroscopy), $CO_2$ (non-dispersive infra red), total peroxy nitrates (TDLIF), PAN (CIMS), black carbon (soot photometer), and optical/physical properties (optical particle counters, nephelometer, PSAP) have been used in this study. More details about principal investigators involved in these measurements as well as instrument specifications are available in the overview paper by Jacob et al. (2010).

Where appropriate we have used a number of chemical filters to remove or minimize confounding factors. Where possible, stratospheric influences were removed using a combination of observed characteristics (water vapor $< 50$ ppm, CO $< 50$ ppb, and $O_3 > 100$ ppb). About 13% of the data in ARCTAS-A and 7% in ARCTAS-B were removed as predominantly stratospheric. A combination of tracers such as CO, $CH_3CN$, halocarbons, and aerosols were used to identify anthropogenic and biomass burning (BB) sources. Air mass ages were qualitatively estimated from observed chemical ratios such as $NO_x/NO_y$, $C_2H_2/CO$ and toluene/benzene as well as from trajectory analysis. Two 3-D chemical transport models (CTMs) namely GEOS-Chem (Zhang et al., 2008; Mao et al., 2010), MOZART (Emmons et al., 2010) and a box model (Olson et al., 2004) simulated ARCTAS observations along the DC-8 flight tracks and have been employed here for purposes of data interpretation and model evaluation. A third high resolution CTM provided simulations for ARCTAS-CARB flights only (CMAQ V4.6, www.cmaq-model.org; Appel et al., 2007).

### *3.1. Long-range pollution transport and influences on Arctic/sub-Arctic composition*

Long-range transport of pollution to high latitudes from Europe, Asia and North America was observed in both phases of ARCTAS

(Fuelberg et al., 2010; Warneke et al., 2009; Fisher et al., 2010). In spring, Eurasian industrial emissions were transported to the region principally in the lower troposphere. The majority of the plumes sampled at higher altitudes (4–8 km) had strong signatures of biomass combustion indicated by elevated mixing ratios of tracers such as $CH_3CN$ and HCN. In ARCTAS-A and B, plumes from boreal fires originating in Siberia were sampled some 3–8 days later at typical altitudes of 4–10 km. In the summer there were far greater impact from Canadian boreal fires impacting the lower troposphere.

An example of transported pollution in the middle and upper troposphere during a mission to the North Pole on July 9, 2008 is shown in Fig. 1 as indicated by elevated mixing ratios of $CH_3CN$, CO and PAN. Ten day back trajectory analysis suggests transported forest fire emissions at around 5 km (84N, 289W) likely originated in southern Russia where wild fires were observed by the MODIS satellite (Fuelberg et al., 2010). Sandwiched between this and the stratosphere was evidence of anthropogenic pollution with possible origins in eastern Asia. Unlike several tracers (e. g. CO, $CH_3CN$) and secondary organics (e. g. PAN), $O_3$ was not distinctly elevated, most likely due to the extremely low availability of $NO_x$ (Fig. 1) at these cold temperatures with reactive nitrogen favorably partitioned into the PAN reservoir (Jacob et al., 1992; Singh et al., 1992, 2007).

The mean composition of the atmosphere at high latitudes was perturbed by episodes of pollution during ARCTAS-A and B. The average vertical structure of a number of selected primary and secondary chemicals under clean conditions (lower quartile CO), all data, and polluted conditions (upper quartile CO); and the observed mean aerosol composition in ARCTAS is shown in Figs. 2 and 3, respectively. Changes in CO are indicative of both anthropogenic and BB sources while those in $CH_3CN$ are only indicative of BB sources. Aerosol composition provides additional information on the sources of pollution. During spring (ARCTAS-A), there was a substantial enhancement above background in CO, PAN, and organic aerosol in the middle troposphere suggesting that BB pollution contributed significantly. In much of the mid to low troposphere (0–7 km) sulfate concentrations were also elevated indicating industrial pollution (Fig. 3a). These were likely also responsible for background black carbon mixing ratios in spring to be larger than in summer. Contrary to the conventional view, there was little indication that nearly all pollution in spring was from industrial sources and remained in the surface layer (Rahn, 1981; Quinn et al., 2007). Mid-tropospheric perturbations from wild fires as well as industrial emissions exceeded those near the surface. In the summer, the atmosphere was significantly more impacted with largest perturbations in the lower troposphere (Fig. 2e–h). The CO vertical structure was nearly identical to that of $CH_3CN$ further suggesting that Canadian boreal fire emissions played a dominant role. Organic aerosol was a main component of BB aerosol emissions (Fig. 3b).

### 3.2. *Reactive nitrogen*

For photochemical simulations to be meaningful it is important that $NO_x$ and its reservoir species be fully characterized (Olson et al., 2004; Singh et al., 2007; Monks et al., 2009). In ARCTAS, the DC-8 carried a full suite of instrumentation to measure all major components of reactive nitrogen namely, $NO_x$, $NO_y$, $HNO_3$, total peroxy nitrates (PNs), total alkyl nitrates, and speciated PANs. As is evident from Fig. 4, the overall reactive nitrogen budget was well balanced with individually measured groups accounting for 90–100% of the total measured reactive nitrogen ($NO_y$). Peroxy nitrates (mostly in the form of PAN) dominated the reactive N budget in both spring (70%) and summer (60%) at high latitudes with a smaller 20% contribution over California. The high fraction of PAN in the cold Arctic supports previous observations in this region and is consistent with high stability of PAN at extremely cold temperatures (Singh et al., 1994; Stroud et al., 2003). $NO_x$ abundance constituted a smaller $NO_y$ fraction of 5% in spring, 10% in summer (ARCTAS-B) and 20% over California. Nitric acid at 40% was the dominant component during ARCTAS-CARB and a minimal fraction (5%) in the Arctic spring. In the upper troposphere (7–12 km), $HNO_3$ was extremely low during all three campaigns averaging between 20 and 40 ppt. Reactive nitrogen was thus well characterized making it a highly valuable data set to test photochemical theory as well as performance of models.

### 3.3. *Ozone*

A key aim of ARCTAS was to investigate the impact of industrial and biomass burning pollution transported to the high northern latitudes on $O_3$ concentrations. Fig. 5 presents a plot of $O_3$ as a function of CO and $CH_3CN$ for ARCTAS-A, ARCTAS-B, and ARCTAS-CARB. Relatively fresh BB plumes at low altitudes (0–3 km) typically encountered during boreal fires in the summer (Fig. 5b) contained very little enhancement in ozone. In the spring where most BB plumes were aged and present in the mid to upper troposphere (5–8 km) a greater enhancement in $O_3$ was observed ($\Delta O_3/\Delta CO = 0.11 \pm 0.09$ v/v). Over California (Fig. 5c) the situation was

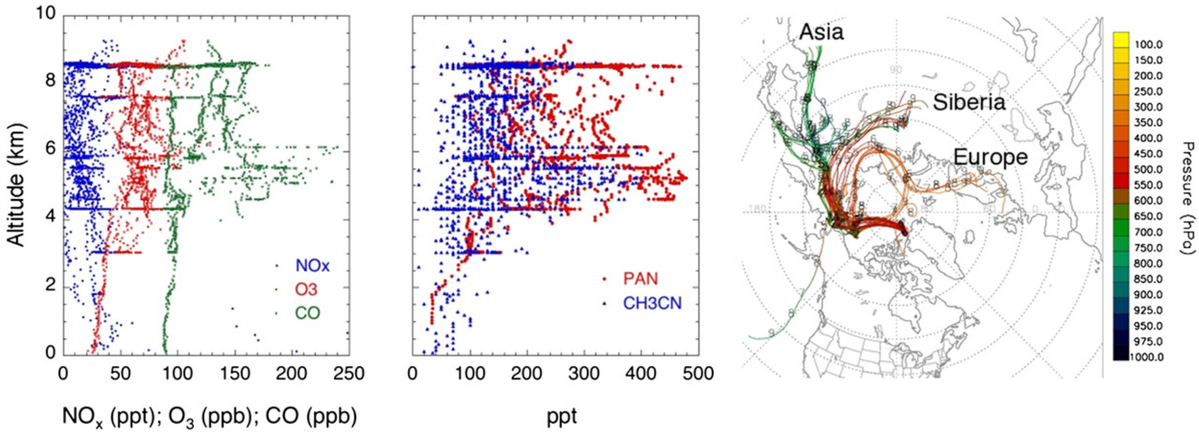

**Fig. 1.** Transport of pollution to the Arctic (>80N) upper troposphere from wild fires in Siberia and anthropogenic pollution in eastern Asia. As sampled by the DC-8 on 9 July 2008. Left two boxes show vertical profiles of a number of key tracers and secondary products; the right hand shows 10-day back trajectories starting at 5 km.

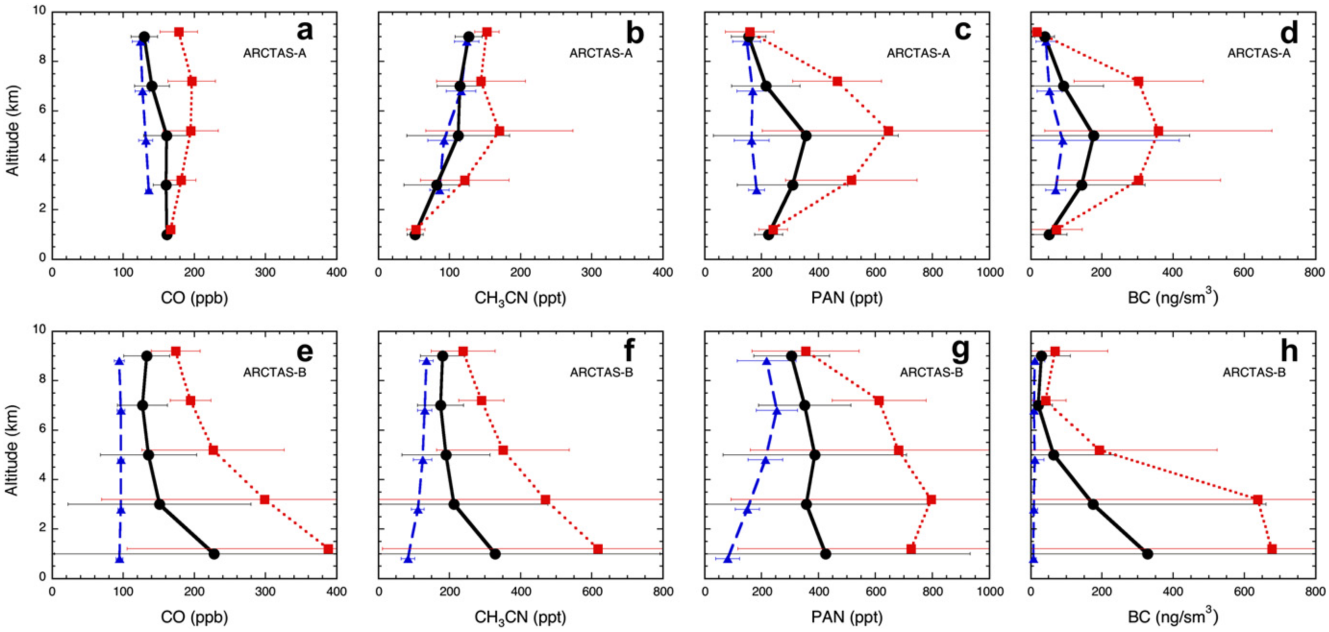

**Fig. 2.** Distribution of selected primary and secondary species at high latitudes during ARCTAS. Top boxes are from ARCTAS-A (spring) and bottom ones from ARCTAS-B (summer). Solid (black) line is a mean of all observed data; dashed (blue) line represents near background conditions (lowest CO quartile) and dotted (red) line represents polluted conditions (highest CO quartile). (For interpretation of the references to colour in this figure legend, the reader is referred to the web version of this article.)

similar in fresh BB plumes but air masses were frequently mixed with urban emissions that offered the opportunity for large $O_3$ formation in the lower troposphere. In the middle and lower troposphere the highest $O_3$ levels occurred under dominant anthropogenic influences. The extremely high $O_3$ levels ($>$120 ppb) in the Arctic/sub-Arctic (Fig. 5a, b) were nearly all in the UT (8–12 km) where polluted air (high CO and PAN) was often mixed with stratospheric air. In California (Fig. 5c) the extremely high $O_3$ levels were in the lower troposphere ($\sim$1 km above ground) east of Fontana. This was an urban fire plume that mixed with anthropogenic emissions at the fire. As a result, the plume contained high $O_3$ levels while the near-by surface monitors (presumably not impacted directly by the fire plume) did not record these. All other fire plumes observed in California had $O_3$ levels less than 100 ppb.

Fig. 6a, b shows the vertical distribution of $O_3$ for spring and summer for high latitudes as a function of the degree of pollution as described in Fig. 2. A comparison of the background profile with all data indicates that transported pollution had at best a small impact on $O_3$. In spring when pollution was transported long distance and aged, the air masses had on average about 10 ppb more ozone than background. However, there were not enough impact and the mean $O_3$ profile was minimally perturbed ($<$5 ppb) compared to background. In summer much of the pollution was relatively fresh and there was little indication of enhanced $O_3$. Plotted in Fig. 6c, d are results based on simulations from GEOS-Chem and MOZART that correspond to the observed behavior shown in Fig. 6a, b. These simulations further support little net impact on mean $O_3$ levels resulting from pollution events. We have selected to show GEOS-Chem for spring (Fig. 6c) and MOZART for summer (Fig. 6d) as these more accurately simulated $NO_x$ (see Fig. 8b, d) necessary for accurate $O_3$ prediction. Thus direct observations and models are consistent in indicating that pollution transport did not provide sufficient precursors for significant changes in mean $O_3$ abundances in the Arctic region. Individual plumes however did contain substantial enhancements in $O_3$ that may impact air quality in certain regions for short periods of time (Oltmans et al., in press).

It was possible to compute production and destruction rates of $O_3$ from direct observations of free radicals ($OH/HO_2$) and nitrogen oxides using the chemically detailed box model of Olson et al. (2004). During the spring campaign (ARCTAS-A) the net $O_3$ production rates (formation–destruction) in the entire troposphere

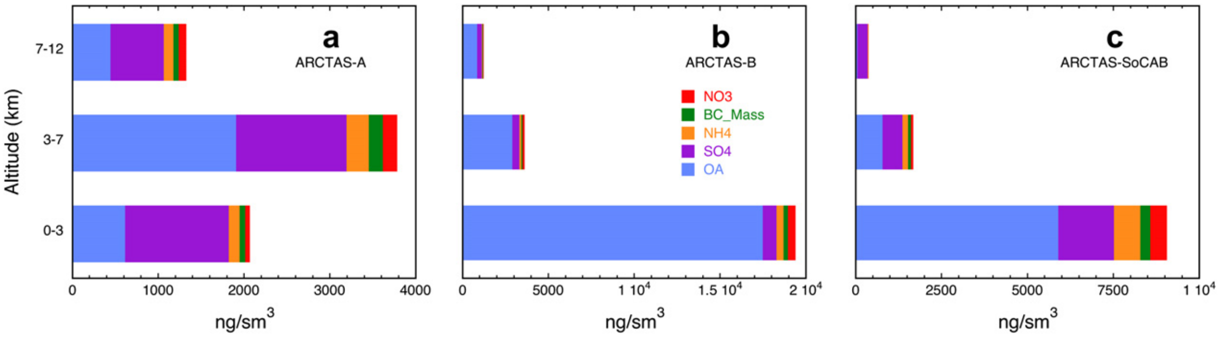

**Fig. 3.** Aerosol composition during ARCTAS. Data are from Aerosol Mass Spectrometer (AMS) measurements on the DC-8.

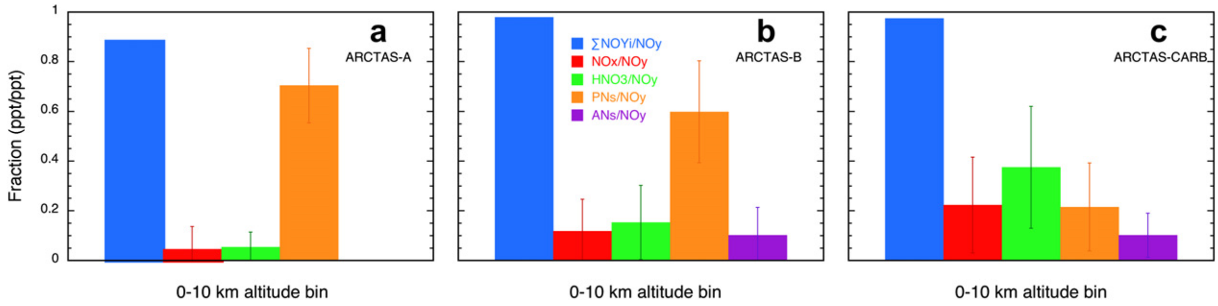

**Fig. 4.** Reactive nitrogen distribution and budget during ARCTAS. Individually measured reactive nitrogen species or groups are plotted as a fraction of total measured nitrogen ($NO_y$) as indicated in (b). The sum of peroxy nitrates (mostly PANs) and alkyl nitrates (ANs) are from UCB-TDLIF; $HNO_3$ is from CIT-CIMS; $NO_x$ and $NO_y$ are from NCAR-chemiluminescent instrument.

was nearly zero (Fig. 7). In the summer season (ARCTAS-B) there was some net $O_3$ production in the lower and upper troposphere ($\approx$0.1 ppb $h^{-1}$). These rather small computed rates of net $O_3$ production further support the observed $O_3$ behavior at high latitudes. In comparison, the BL over California (0–2 km) showed significant net $O_3$ production with median values approaching 1.5 ppb $h^{-1}$. In all cases there was evidence of net $O_3$ destruction ($<-0.1$ ppb $h^{-1}$) in the middle troposphere (2–8 km).

### 3.4. Models of transport and chemistry and comparisons with observations

A comparison between observations and model simulations for $O_3$ and $NO_x$ for the three ARCTAS phases is presented in Fig. 8. The potential upper limit error in $NO_x$ measurements due to $CH_3OONO_2$ decomposition is also shown. Depending on the model, high latitude $NO_x$ is both under-predicted and over-predicted with little direct relation to ozone prediction (Fig. 8a–d). In ARCTAS-A, GEOS-Chem simulates $NO_x$ more accurately than MOZART (Fig. 8b) but the reverse is the case for $O_3$ (Fig. 8a). Similarly, $NO_x$ simulated by GEOS-Chem in ARCTAS-B (Fig. 8d) is substantially larger than MOZART although $O_3$ predictions are similar (Fig. 8c). While models are able to simulate mean $O_3$ to within 20 ppb at high latitudes there is little internal consistency in this behavior. A large part of this disagreement comes from difficulties in correctly simulating $NO_x$ and exchange with the stratosphere. The agreement for data over California was generally superior for all three models (Fig. 8e, f). It is noted that the CMAQ model for California did not contain any fire emissions and yet predicted $NO_x$ and $O_3$ as accurately as models that did. This is in accordance with the observation that relatively fresh fire emissions lack significant amounts of $NO_x$ and thus are not conducive to significant ozone formation.

Fig. 9 shows comparisons between observations and models for a select group of primary and secondary gases and aerosols measured during ARCTAS-A and ARCTAS-B. The selected species (acetone, PAN, $HNO_3$, and $SO_4^{-}$) cover a wide range of sources as well as atmospheric characteristics (e. g. chemistry, solubility) and can provide a reasonable test for the overall ability of selected models. It is evident that there are fairly large uncertainties in the ability of models to simulate observed high latitude composition. The rather large disagreements between Arctic black carbon observations and model simulation have been previously reported by Shindell et al. (2008). Some of the differences are probably due to errors in emission inventories (e. g. acetone) while others are due to poor simulations of chemistry and/or removal during transport (e. g. PAN, $HNO_3$, $SO_4^{-}$). We also note that model-to-model deviations can often exceed those with observations. To date, much of the data available from the Arctic region has been from surface sites only. While global models capture the broad distribution of chemicals in the Arctic, there has been insufficient 3-dimensional data for their validation and refinement. In this regard the ARCTAS campaign fills a critical need providing opportunities for future model improvements. There is also a clear need for standardized model inter-comparisons to determine the causes of disagreements among models.

### 3.5. BB emissions and urban influences

During ARCTAS-A and -B, MODIS satellite imagery indicated widespread fire activity in Siberia. MODIS data over Siberia from

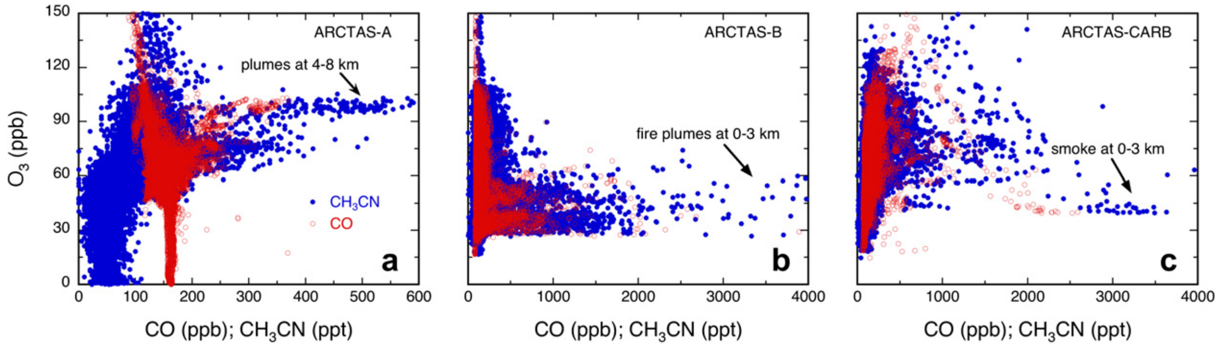

**Fig. 5.** Ozone as a function biomass burning tracer ($CH_3CN$) and general pollution (CO) during ARCTAS. The extremely high $O_3$ values (>120 ppb) in (a) and (b) are all in the upper troposphere associated with polluted air masses that could not be separated from stratospheric influences. $O_3$, CO and $CH_3CN$ are as measured by chemiluminescence, TDLAS and PTR-MS, respectively.

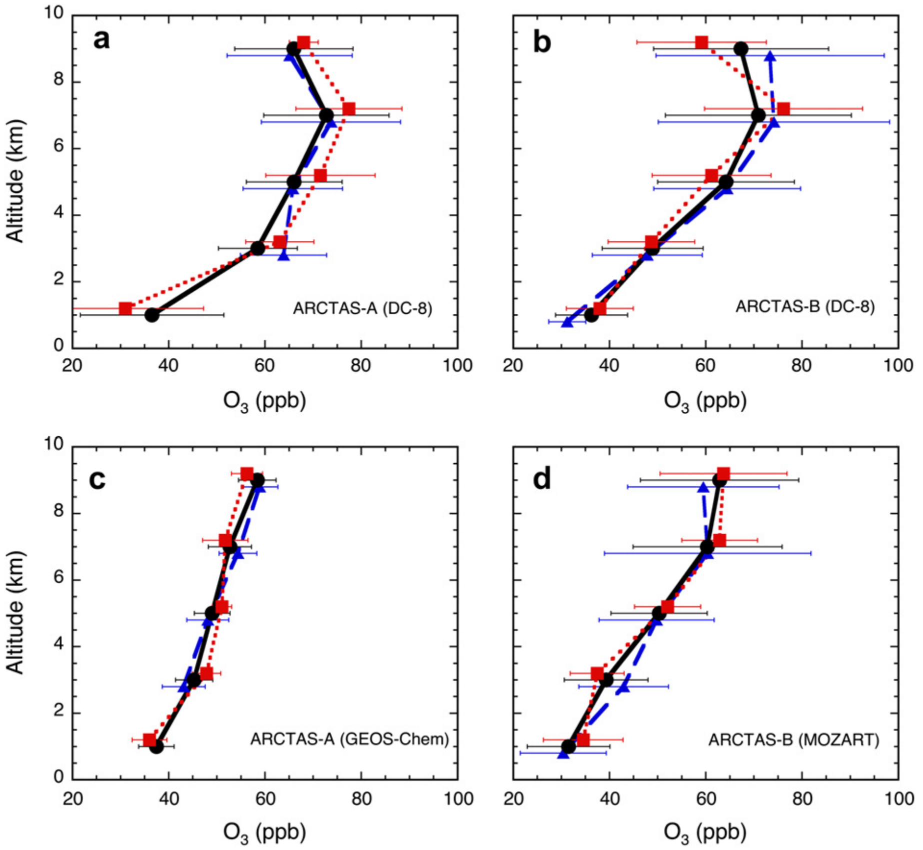

**Fig. 6.** Observed and modeled ozone behavior at high latitudes during spring (ARCTAS-A) and summer (ARCTAS-B). The three lines indicate near background (dashed-blue), polluted (dotted-red), and average observed (solid-black) conditions (as defined in Fig. 2 legend). The top 2 boxes (a, b) are based on DC-8 data; the lower two boxes are simulations using GEOS-Chem (c) and MOZART (d). See text for more details. (For interpretation of the references to colour in this figure legend, the reader is referred to the web version of this article.)

2000 to 2009 indicated that April 2008 fire counts were the highest while the summer peak was second only to 2003. ARCTAS-B (summer) also saw extensive boreal fires burning throughout Canada. In 2008 the Saskatchewan burned area, easily accessible to the DC-8 from its Cold Lake base, significantly exceeded the 20 year average statistics while overall Canadian fires were near normal (Soja et al., 2008). California also experienced one of the largest episodes of wild fires in June 2008, with over a 1000 fires burning, and ARCTAS-CARB took advantage of this unique opportunity to investigate emissions from mid-latitude wild fires and their comparison with boreal fires.

Fig. 10 displays a plot of important greenhouse gases (GHG), oxygenated volatile organic chemicals (OVOC) and $CH_3CN$ (BB tracer) as a function of CO, a well-known indicator of multiple pollution sources. The extensive measurements of tracers on the DC-8 allowed identification of source types (anthropogenic, biogenic, and BB) as noted in Fig. 10. The highest methane concentrations (Fig. 10a) were encountered over biogenic/agricultural fields (typically low CO and $CH_3CN$), with urban emissions next ($\Delta CH_4/\Delta CO \approx 1$ v/v) and the lowest rate of emission from BB sources ($\Delta CH_4/\Delta CO \approx 0.08$ v/v). It is evident from Fig. 10a that the $CH_4$ BB emission rates for the three regions were very nearly identical. Enhancements of $CO_2$ ($\Delta CO_2/\Delta CO$) from urban pollution of nearly 100 v/v far exceeded those from BB (10 v/v). Nitrous oxide was negligibly elevated in BB plumes ($\Delta N_2O/\Delta CO \approx 0.001$ v/v) with larger contributions from agricultural and anthropogenic sources. Relative enhancements of a variety of OVOC in BB plumes sampled in the three phases of ARCTAS were very similar (Fig. 10d–f). It did appear that the $CH_3CN$ enhancement in California fires was somewhat lower than boreal fires. This difference is likely due to the variations in biomass composition and the different flaming/smoldering balance in these fires.

Some 70 small and large pollution plumes were identified during ARCTAS. Using CH3CN as a BB tracer, 18 plumes were

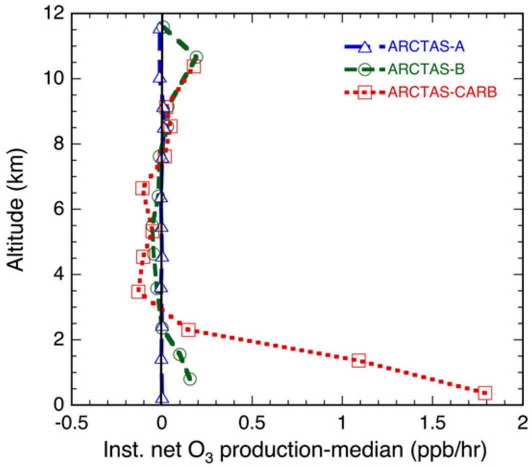

**Fig. 7.** Median net ozone production rates from the three ARCTAS phases. These are constrained by chemical and physical parameters measured by the DC-8 and calculated using the NASA Langley box model (Olson et al., 2004).

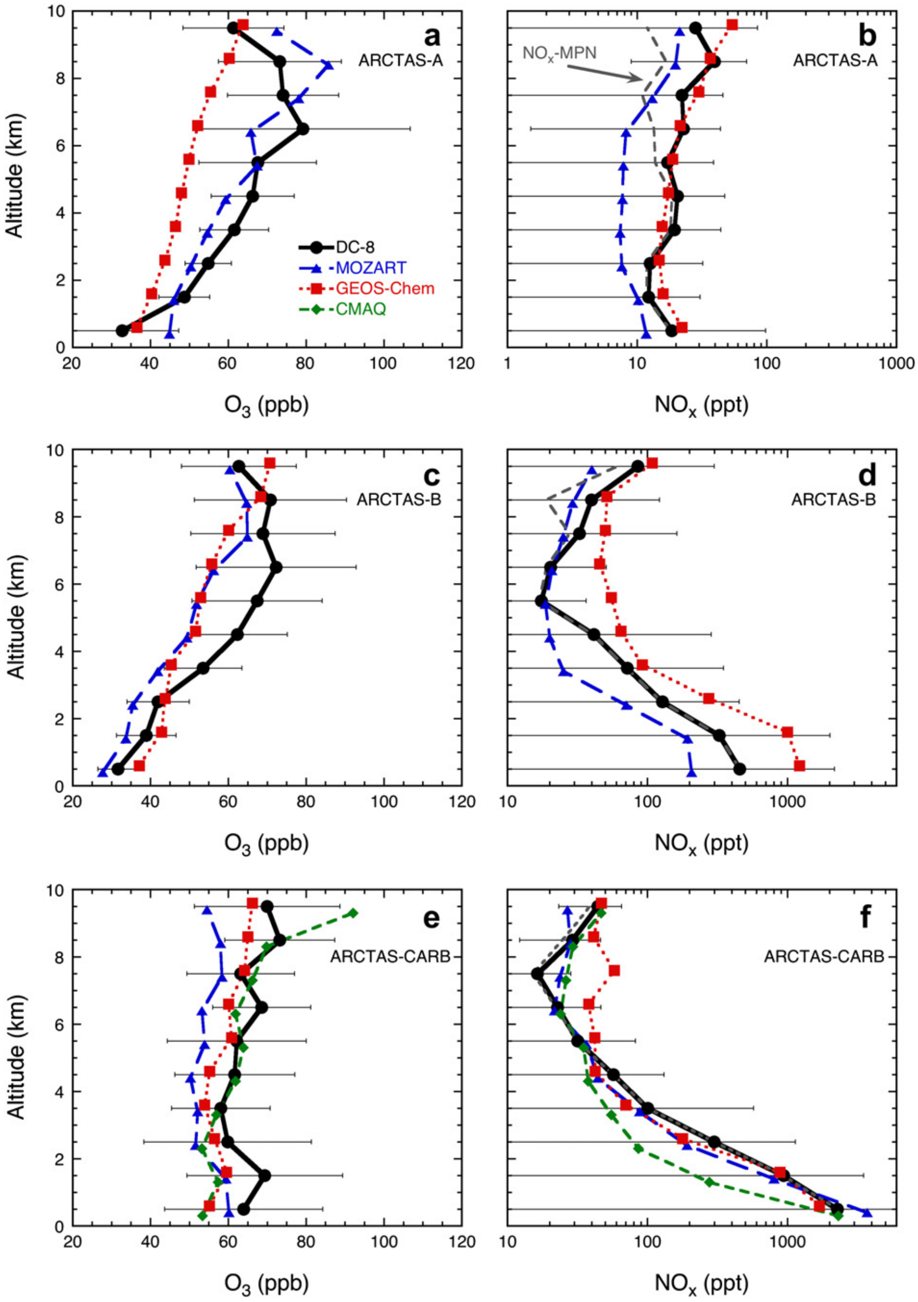

**Fig. 8.** Mean tropospheric profiles of observed and modeled $O_3$ and $NO_x$. MOZART and GEOS-Chem simulations are shown for all phases of ARCTAS. CMAQ model runs were available only for ARCTAS-CARB and did not incorporate fire emissions. $NO_x$-MPN line indicates $NO_x$ when corrected for maximum possible $CH_3OONO_2$ interference. Ozone and $NO_x$ data are from the NCAR-chemiluminescent instrument.

identified as fresh BB plumes mostly present in the lower troposphere (2 ± 2 km). Twenty plumes sampled in the middle to upper troposphere (7 ± 2 km) were transported from Eurasian regions and contained both anthropogenic and biomass burning signatures. Twelve plumes were identified as mainly of anthropogenic origin (elevated CO and no enhancement in $CH_3CN$) present largely over California at low altitudes. In Table 1 we provide mean enhancements of a variety of species relative to CO in these selected plumes. We note that given the long lifetime of CO in the middle troposphere (3–4 months) it can be treated as a nearly inert tracer during the 1–7 day transport time associated with these plumes. The Modified Combustion Efficiency $\{(1+\Delta CO/\Delta CO_2)^{-1}\}$ of 0.94 in transported plumes (column 2) can be compared with 0.90 in fresh BB plumes (column 1) and 0.99 in urban plumes (column 3) suggesting that high altitude transported pollution contained both BB and urban influences.

Enhancement ratios of plumes that were identified to have predominantly BB signatures (column 1) were in general agreement with data reported in Fig. 10. Mean relative enhancements of several species such as $CO_2$, $CH_4$, methanol, acetone, benzene, toluene and aerosol are comparable to those observed at locations and in other studies (Goode et al., 2000; de Gouw et al., 2006; de Gouw and Jimenez, 2009; Mieville et al., 2010). The most distinct features of BB plumes when compared to anthropogenic air masses was rather low relative enhancements in $CH_4$, $CO_2$, and $N_2O$ and rather high enhancements in organic aerosol (Fig. 11). Nine plumes

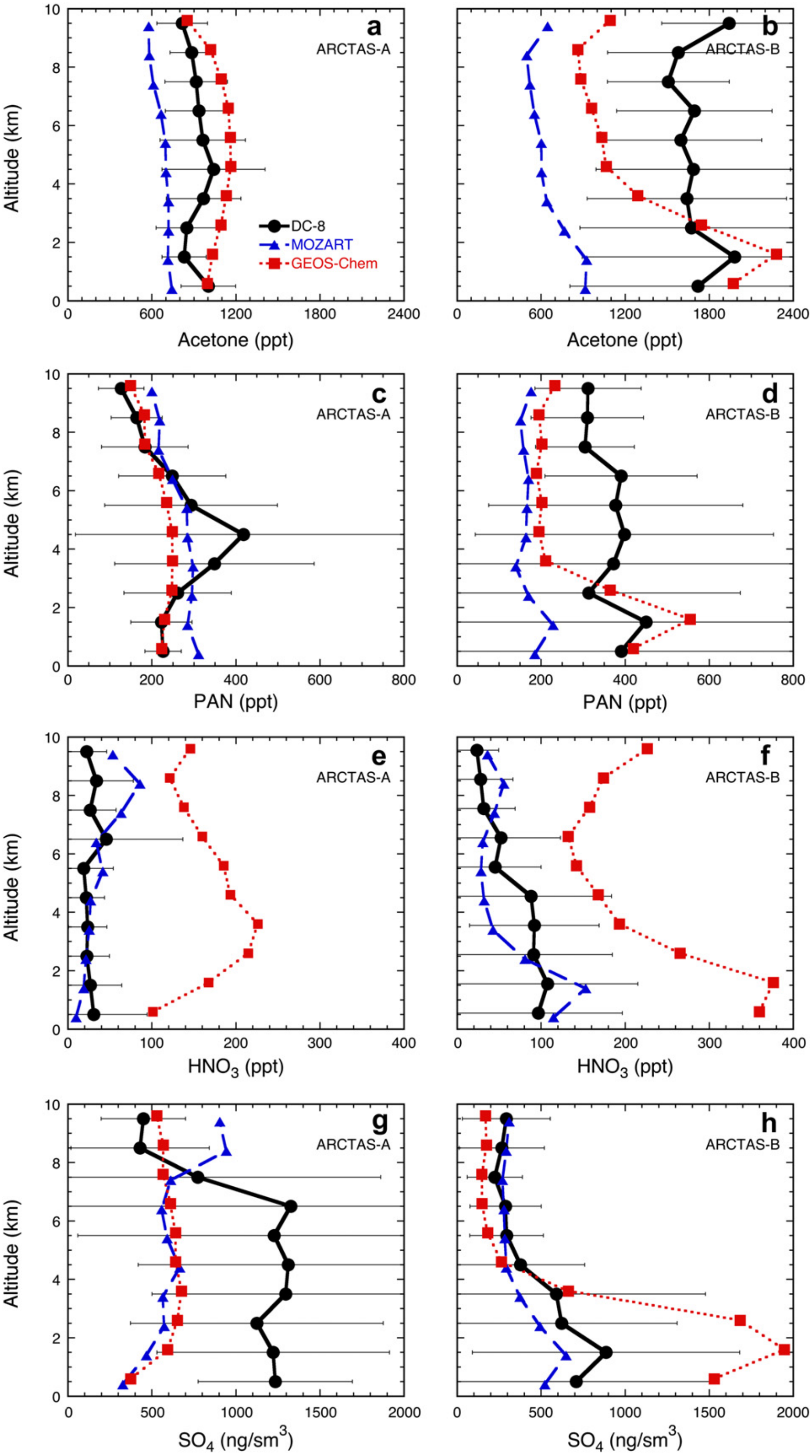

**Fig. 9.** Observed and modeled concentrations of selected primary and secondary constituents at high latitudes (>50N) during ARCTAS. MOZART and Geos-Chem results are shown in dashed (blue) and dotted (green) lines as in Fig. 8. (For interpretation of the references to colour in this figure legend, the reader is referred to the web version of this article.)

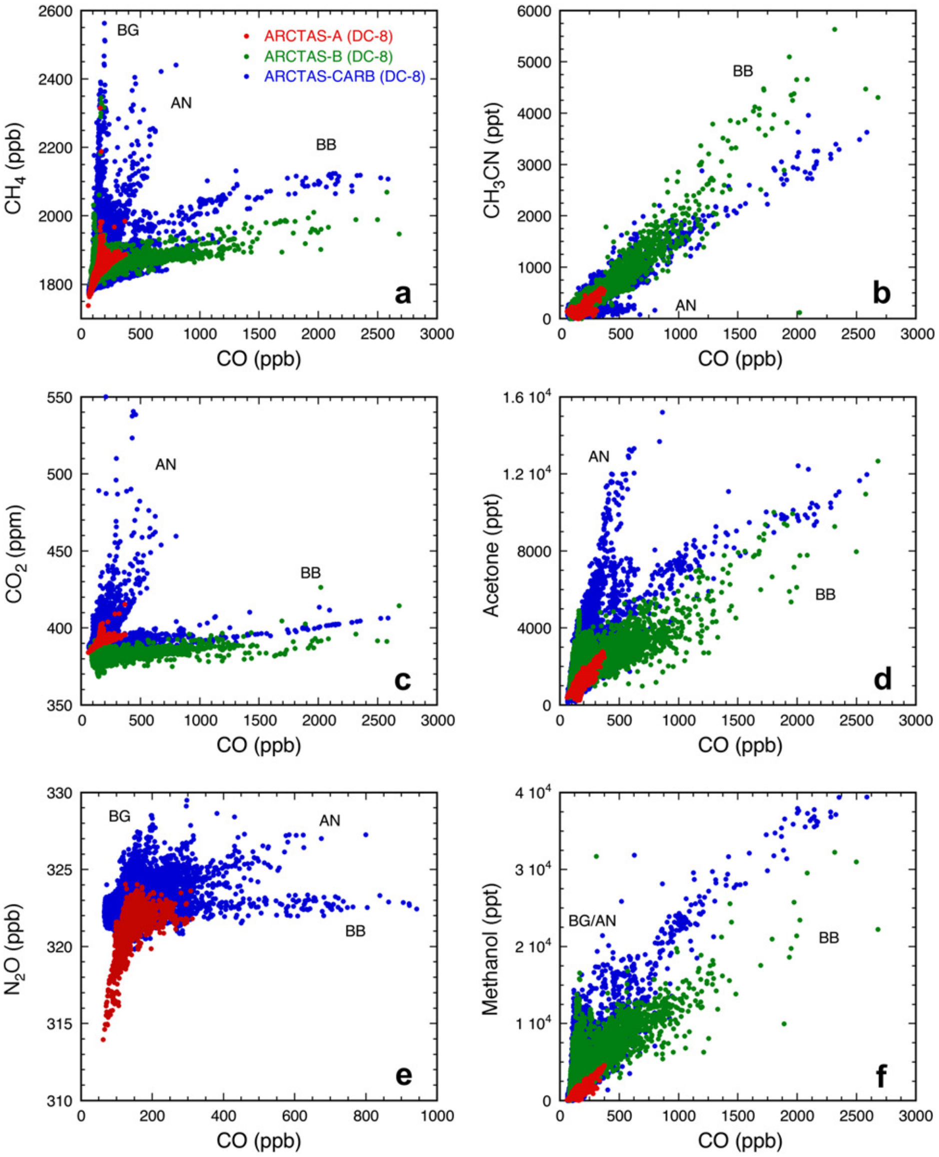

**Fig. 10.** Relationship of selected greenhouse gases and organic chemicals with carbon monoxide tracer for the three phases of ARCTAS. BB: biomass burning, AN: anthropogenic; BG: biogenic. Data sources as described in text.

measured in Arctic spring were greatly enhanced in BC ($\Delta BC/\Delta CO = 9.4 \pm 3.3$ ng sm$^{-3}$ ppb$^{-1}$) and $SO_4^{--}$ ($\Delta SO_4/\Delta CO = 29 \pm 19$ ng sm$^{-3}$ ppb$^{-1}$) indicating greater industrial influences in ARCTAS-A (Table 1). As has been suggested previously, it also appears from Table 1 that unlike $CH_3CN$, HCN may also have anthropogenic sources that are presently not well quantified (Singh et al., 2003; Baum et al., 2007; Crounse et al., 2009).

Organic aerosol, black carbon, CO and PAN enhancements in BB plumes increased linearly with $\Delta CH_3CN$. However, this was not the case for $O_3$ whose enhancement in plumes was not easily discernible and was often uncorrelated with $\Delta CH_3CN$. Relatively fresh plumes of BB origin (column 1) had little $NO_x$ and minimal $O_3$ enhancement ($\Delta O_3/\Delta CO = 0.03 \pm 0.04$ v/v). A comparison of emission ratios in various plume types (columns 1–3) of Table 1 suggests that most of the plumes at high altitudes had some urban pollution in them. As an example $\Delta CH_4/\Delta CO$ and $\Delta SO_4/\Delta CO$ can be seen to increase significantly with greater anthropogenic influences. More aged BB plumes that also contained some urban pollution were substantially enhanced in $O_3$ ($\Delta O_3/\Delta CO = 0.11 \pm 0.09$ v/v). These relative responses indicate similarities in fire emissions from widely different regions and their change with increasing anthropogenic pollution.

Enhancements of species relative to CO in urban plumes (Table 1 and Fig. 10) in many cases are useful in assessing the accuracy of emission inventories generally derived from bottom-up data. This is particularly true for greenhouse gas emissions that are presently being quantified in many regions of the world. Here we use data from the urban plumes shown in Table 1 to assess the emissions information for $CH_4$ and $N_2O$. We note that the CARB CO emission inventory (http://www.arb.ca.gov/app/emsinv/emssumcat.php) for all California and South Coast Air Basin (SoCAB) indicating CO emissions of 4.1 Tg y$^{-1}$ and 1.2 Tg y$^{-1}$, respectively is in reasonably good agreement with ARCTAS-CARB observations and has been extensively validated by the state. Bottom-up $CH_4$ emissions for the entire CA state (http://www.arb.ca.gov/cc/inventory/data/data.htm) are estimated to be 1.3 Tg y$^{-1}$ with about 56% coming from the agricultural sources. Scaling this emission inventory to the SoCAB region (50% population/5% agricultural), we estimate a $CH_4$

**Table 1**
Enhancement ratios of selected species relative to CO in a variety of pollution plumes sampled during ARCTAS.

| Enhancement ratios relative to CO | Fresh BB plumes (alt. 2.0 ± 1.3 km)[a] | Aged BB/urban plumes (alt. 6.9 ± 2.0 km)[b] | Urban plumes (alt. 1.6 ± 2.5 km)[c] | Estimated global BB source[d] (Tg y$^{-1}$) |
|---|---|---|---|---|
| $\Delta CH_3CN/\Delta CO$ (ppt ppb$^{-1}$) | 2.0 ± 0.5 | 2.6 ± 0.5 | 0.0 ± 0.0 | 1.0 |
| $\Delta HCN/\Delta CO$ (ppt ppb$^{-1}$) | 5.6 ± 3.0 | 7.5 ± 2.1 | 1.5 ± 1.2 | 2.0 |
| $\Delta CH_4/\Delta CO$ (ppb ppb$^{-1}$) | 0.08 ± 0.03 | 0.25 ± 0.10 | 1.1 ± 1.1 | 17.1 |
| $\Delta CO_2/\Delta CO$ (ppb ppb$^{-1}$) | 9.4 ± 3.7 | 15.4 ± 17.3 | 109 ± 80 | 5539 |
| $\Delta O_3/\Delta CO$ (ppb ppb$^{-1}$) | 0.03 ± 0.04 | 0.11 ± 0.09 | 0.09 ± 0.11 | – |
| $\Delta NO_y/\Delta CO$ (ppt ppb$^{-1}$) | 8.3 ± 4.1 | 9.9 ± 8.3 | 137 ± 145 | 1.6[e] |
| $\Delta NO_x/\Delta CO$ (ppt ppb$^{-1}$) | 3.5 ± 4.2 | 0.9 ± 1.5 | 123 ± 113 | 0.7[e] |
| $\Delta HNO_3/\Delta CO$ (ppt ppb$^{-1}$) | 0.3 ± 0.6 | 0.3 ± 0.4 | 14.5 ± 11.8 | 0.1[e] |
| ΔPAN/ΔCO (ppt ppb$^{-1}$) | 2.7 ± 1.8 | 4.1 ± 3.1 | 5.6 ± 4.1 | 0.5[e] |
| ΔHCHO/ΔCO (ppt ppb$^{-1}$) | 15.8 ± 7.8 | 3.7 ± 4.2 | 23.0 ± 13.7 | 6.3 |
| $\Delta CH_3OOH/\Delta CO$ (ppt ppb$^{-1}$) | 13.4 ± 16.2 | 6.7 ± 8.6 | 6.2 ± 6.2 | 8.6 |
| $\Delta CH_3OH/\Delta CO$ (ppt ppb$^{-1}$) | 15.6 ± 9.2 | 21.1 ± 7.0 | 21.0 ± 14.0 | 6.7 |
| $\Delta CH_3COCH_3/\Delta CO$ (ppt ppb$^{-1}$) | 4.7 ± 3.3 | 10.6 ± 3.6 | 18.3 ± 9.5 | 3.6 |
| $\Delta CH_3CHO/\Delta CO$ (ppt ppb$^{-1}$) | 4.9 ± 3.3 | 2.4 ± 2.0 | 4.4 ± 2.6 | 2.9 |
| $\Delta C_7H_8/\Delta CO$ (ppt ppb$^{-1}$) | 0.7 ± 0.2 | 0.8 ± 0.5 | 2.3 ± 1.3 | 0.9 |
| $\Delta C_6H_6/\Delta CO$ (ppt ppb$^{-1}$) | 1.6 ± 0.3 | 2.0 ± 0.4 | 1.6 ± 0.3 | 1.6 |
| $\Delta SO_2/\Delta CO$ (ppt ppb$^{-1}$) | 1.1 ± 0.6 | 0.6 ± 1.5 | 30 ± 35 | 1.0 |
| $\Delta SO_4/\Delta CO$ (ng sm$^{-3}$ ppb$^{-1}$) | 3.0 ± 1.7 | 11.6 ± 17.2 | 29 ± 33 | 0.9 |
| $\Delta NO_3/\Delta CO$ (ng sm$^{-3}$ ppb$^{-1}$) | 6.3 ± 3.5 | 3.3 ± 4.3 | 7.6 ± 7.9 | 1.9 |
| ΔBC/ΔCO (ng sm$^{-3}$ ppb$^{-1}$) | 1.6 ± 0.9 | 2.4 ± 2.8 | 2.4 ± 0.5 | 0.5 |
| ΔOA/ΔCO (ng sm$^{-3}$ ppb$^{-1}$) | 155 ± 60 | 60 ± 60 | 40 ± 25 | 46.0 |

[a] Moderately fresh near source BB plumes (N = 18; $\Delta CH_3CN = 2.4 \pm 1.5$ ppb).

[b] Moderately aged (1–5 days) BB plumes (N = 20; $\Delta CH_3CN = 0.3 \pm 0.1$ ppb) transported from long distances are mixed with anthropogenic pollution. In ARCTAS-A (April) mean $SO_4$ and BC enhancements in nine sampled plumes were comparable to or larger than those in fresh urban plumes.

[c] Urban pollution plumes (N = 11; $\Delta CH_3CN = 0.0 \pm 0.0$ ppb) mainly sampled over California.

[d] Based on mean data in column 1 and a global BB CO emission rate of 375 Tg y$^{-1}$ (see text). Does not include biofuel or charcoal burning.

[e] Expressed in units of Tg(N) y$^{-1}$.

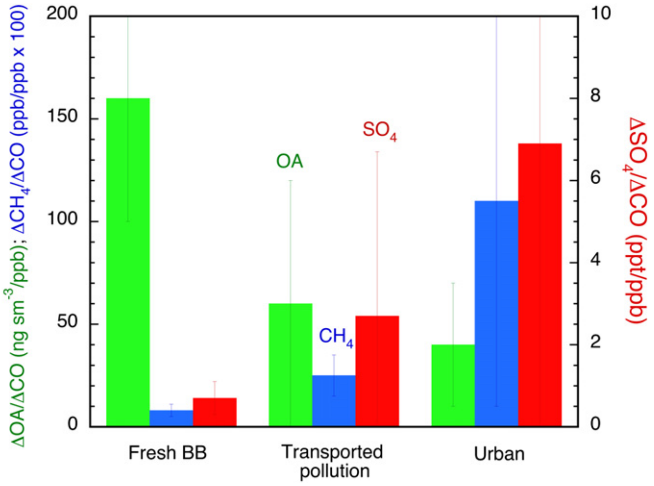

**Fig. 11.** Enhancements of organic aerosol (OA), methane ($CH_4$) and fine sulfate ($SO_4$) relative to CO as a function of plume types. For more detail see Table 1.

source of about 0.35 Tg y$^{-1}$. However, using the mean $\Delta CH_4/\Delta CO$ ratio of approx 1 v/v measured over southern California in urban plumes would suggest a SoCAB $CH_4$ source of 0.7 Tg y$^{-1}$ or nearly twice as large. A similar analysis for $CO_2$ and $N_2O$ leads to SoCAB emission estimate of 200 Tg y$^{-1}$ and 0.02 Tg y$^{-1}$ respectively, in reasonable agreement with the state inventory. The anthropogenic emission rate of $N_2O$ in California is low in large part due to the use of low sulfur fuels (Graham et al., 2009). Emissions rates of $N_2O$ are likely to be larger in urban centers around the world with higher fuel sulfur content. We also note that ground based observations of Hsu et al. (2010) disagree with ARCTAS-CARB data and report a $\Delta CH_4/\Delta CO$ of only 0.5 v/v, resulting in good agreement with the bottom-up state inventory. Clearly many uncertainties are present and additional observational data are necessary for satisfactory validation of GHG emissions in California.

Given that BB emission rates appear to be relatively similar, we use these data to estimate the global BB sources of several species in Table 1 assuming a best available global BB CO source of 375 (±20%) Tg y$^{-1}$ (Van der Werf et al., 2006; revised by −14% as per private communication of authors). These estimates do not include emissions resulting from biofuel and charcoal burning sources. Where comparisons are possible, these global estimates are in reasonably good agreement with previously published data (Andreae and Merlet, 2001; Singh et al., 2003, 2004; de Gouw et al., 2006; Schultz et al., 2008; de Gouw and Jimenez, 2009; and references therein).

### 3.6. Optical effects

The DC-8 also measured detailed aerosol composition as well as their physical and optical properties. Fig. 12a shows a plot of ARCTAS-CARB submicron scattering and total absorption at 532 nm (green) as a function of degree of pollution represented by CO. The relationship with black carbon was nearly identical. It is evident that BB aerosol were strongly absorbing and both absorption and scattering increased nearly linear as a function of CO. This relationship was also observed in boreal forest plumes with nearly identical behavior. Fig. 12b shows the behavior of single scattering albedo (scattering/absorption + scattering; SSA), a quantity necessary for satellite aerosol retrievals, that had a mean value of 0.93. In ARCTAS-B, SSA declined from about 0.94 to 0.91 (more absorbing) with increasing BB smoke. Over California this behavior was reversed with lower SSA at lower CO concentrations that were associated with greater urban (southern California) influences. Although black carbon concentrations in urban air over California were moderately high, these were lower than those observed in boreal fires. Also BC particles were found to be more thickly coated in fire impacted air than in urban air. We speculate that the greater abundance of organic aerosol, which is more reflective, in BB smoke influenced air (Fig. 3) caused these air masses to have higher SSA than similar concentrations in urban air. In all cases absorption and scattering changed in a near linear fashion as a function of increasing pollution causing SSA to be minimally impacted. Although we only show data for 532 nm, similar relationships were also evident at other wavelengths studied (470 nm and 660 nm).

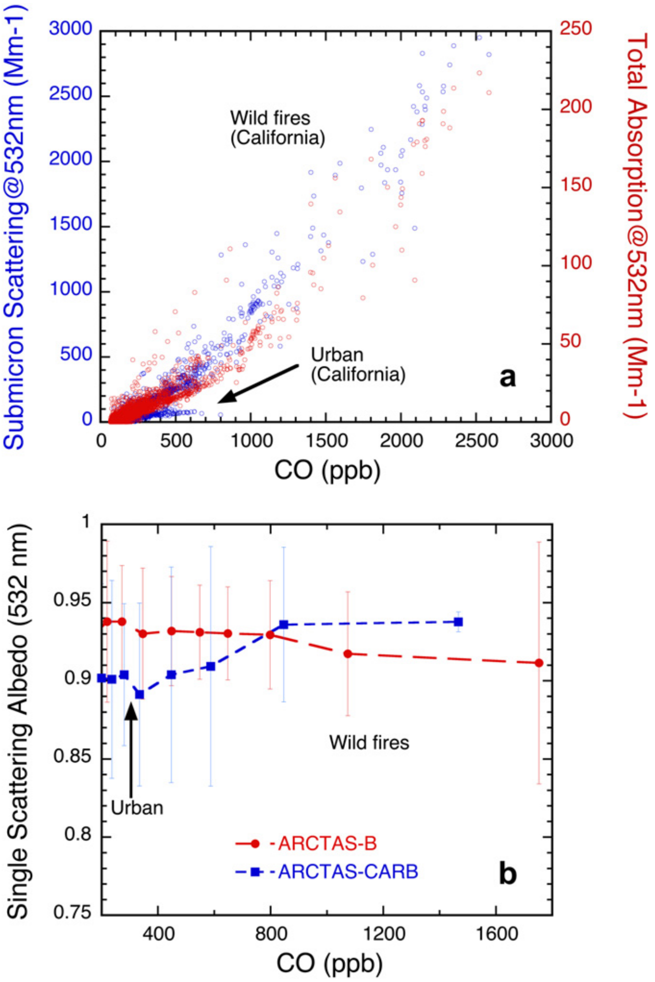

**Fig. 12.** Aerosol optical effects on solar radiation as a function of pollution influences represented by CO. (a) Shows a linear relationship of scattering and absorption as observed over California; (b) shows a comparison of single scattering albedo from California and Canadian fire influences. BB aerosols were thickly coated with organic material. The urban influences were largely based on data acquired over southern California.

Russell et al. (2010) summarize SSA for many different aerosol types that are generally consistent with ARCTAS findings.

## 4. Conclusions

The ARCTAS campaign provided a wealth of three-dimensional data detailing the composition of gases and aerosols over the Arctic and over California. Widespread pollution influences could be detected at high latitudes from transported anthropogenic and BB pollution as well as locally generated pollution from boreal fires. Frequent pollution transport was from the Eurasian regions with occasional incursions from North American. Contrary to the conventional view of Arctic haze as a surface based anthropogenic pollution phenomenon, pollution impacts from anthropogenic and biomass burning sources were seen at all altitudes in the troposphere. Although the mean composition of many constituents, especially aerosols, changed greatly due to pollution this was not the case for ozone, which appeared to change minimally. BB plumes produced significant ozone only when mixed with urban pollution. Boreal as well as California fires had very similar emission characteristics and optical properties. ARCTAS-CARB data also suggest that urban emissions of some greenhouse gases (e. g. methane) may be under estimated in California. ARCTAS provided a unique and extensive body of data set from high latitudes that is useful for further improvements in our knowledge and in model simulations. These data are now available to all interested parties for further analysis and new findings are expected.

## Acknowledgments

The ARCTAS campaign was funded by the NASA Tropospheric Chemistry Program, the NASA Radiation Sciences Program, and the California Air Resources Board. PTR-MS measurements were supported by the Austrian Research Promotion Agency (FFG), the Tiroler Zukunftstiftung, and the University of Innsbruck. We thank all ARCTAS participants for their contributions.

## References

Andreae, M., Merlet, P., 2001. Emissions of trace gases and aerosols from biomass burning. Global Biogeochem. Cycles 15, 955–966.

Appel, K.W., Gilliland, A.B., Sarwar, G., Gilliam, R.C., 2007. Evaluation of the community multiscale air quality (CMAQ) model version 4.5: sensitivities impacting model performance; part I—ozone. Atmos. Environ. 41 (40), 9603–9615.

Barrie, L.A., 1986. Arctic air pollution: an overview of current knowledge. Atmos. Environ. 20 (4), 643–663.

Baum, M.M., Moss, J.A., Pastel, S.H., Poskrebyshev, G.A., 2007. Hydrogen cyanide exhaust emissions from in-use motor vehicles. Environ. Sci. Technol. 41 (3), 857–862.

Clarke, A.D., Noone, K.J., 1985. Soot in the Arctic snowpack: a cause for perturbations of radiative transfer. Atmos. Environ. 19 (12), 2045–2053.

Colarco, P.R., Schoeberl, M.R., Doddridge, B.G., Marufu, L.T., Torres, O., Welton, E.J., 2004. Transport of smoke from Canadian forest fires to the surface near Washington, D.C.: injection height, entrainment, and optical properties. J. Geophys. Res. 109, D06203. doi:10.1029/2003JD004248.

Crounse, J.D., DeCarlo, P.F., Blake, D.R., et al., 2009. Biomass burning and urban air pollution over the Central Mexican Plateau. Atmos. Chem. Phys. 9, 4929–4944.

de Gouw, J.A., Warneke, C., Stohl, A., et al., 2006. Volatile organic compounds composition of merged and aged forest fire plumes from Alaska and western Canada. J. Geophys. Res. 111, D10303. doi:10.1029/2005JD006175.

de Gouw, J., Jimenez, J.L., 2009. Organic aerosols in the Earth's atmosphere. Environ. Sci. Technol. 43, 7614–7618.

Emmons, L.K., Walters, S., Hess, P.G., Lamarque, J.-F., et al., 2010. Description and evaluation of the model for ozone and related chemical tracers, version 4 (MOZART-4). Geosci. Model Dev. 3, 43–67.

Fisher, J.A., Jacob, D.J., Purdy, M.T., et al., 2010. Source attribution and interannual variability of Arctic pollution in spring constrained by aircraft (ARCTAS, ARCPAC) and satellite (AIRS) observations of carbon monoxide. Atmos. Chem. Phys. 10, 977–996.

Flanner, M.G., Zender, C.S., Randerson, J.T., Rasch, P.J., 2007. Present-day radiative forcing and climate response from black carbon in snow. J. Geophys. Res. 112, D11202. doi:10.1029/2006JD008003.

Fromm, M.D., Servranckx, R., 2003. Transport of forest fire smoke above the tropopause by supercell convection. Geophys. Res. Lett. 30 (10), 1542. doi:10.1029/2002GL016820.

Fuelberg, H.E., Harrigan, D.L., Sessions, W., 2010. A meteorological overview of the ARCTAS 2008 mission. Atmos. Chem. Phys. 10, 817–842.

Goode, J.G., Yokelson, R.J., Ward, D.E., et al., 2000. Measurements of excess $O_3$, $CO_2$, CO, $CH_4$, $C_2H_4$, $C_2H_2$, HCN, NO, $NH_3$, HCOOH, $CH_3COOH$, HCHO, and $CH_3OH$ in 1997 Alaskan biomass burning plumes by airborne Fourier transform infrared spectroscopy (AFTIR). J. Geophys. Res. 105 (D17), 22147–22166.

Graham, L.A., Belisle, S.L., Rieger, P., 2009. Nitrous oxide emissions from light duty vehicles. Atmos. Environ. 43 (12), 2031–2044.

Hansen, J., Nazarenko, L., 2004. Soot climate forcing via snow and ice albedos. Proc. Natl. Acad. Sci. U.S.A. 101 (2), 423–428.

Hsu, Y.-K., VanCuren, T., Park, S., Jakober, C., Herner, J., FitzGibbon, M., Blake, D.R., Parrish, D.D., 2010. Methane emissions inventory verification in southern California. Atmos. Environ. 44 (1), 1–7.

IPCC, 2007. The Physical Science Basis. Contribution of Working Group I to the Fourth Assessment Report of the Intergovernmental Panel on Climate Change. Cambridge University Press, New York, USA. Available at http://www.ipcc.ch.

Jacob, D.J., Crawford, J.H., Maring, H., et al., 2010. The ARCTAS aircraft mission: design and execution. Atmos. Chem. Phys. 10, 5191–5212.

Jacob, D.J., Wofsy, S.C., Bakwin, P.S., et al., 1992. Summertime photochemistry at high northern latitudes. J. Geophys. Res. 97 (D15), 16421–16431.

Klonecki, A., Hess, P., Emmons, L., Smith, L., Orlando, J., Blake, D., 2003. Seasonal changes in the transport of pollutants into the Arctic troposphere-model study. J. Geophys. Res. 108 (D4), 8367. doi:10.1029/2002JD002199.

Law, K.S., Stohl, A., 2007. Arctic air pollution: origins and impacts. Science 315 (5818), 1537–1540. doi:10.1126/science.1137695.

Leung, F.T., Logan, J.A., Park, R., et al., 2007. Impacts of enhanced biomass burning in the boreal forests in 1998 on tropospheric chemistry and the sensitivity of model results to the injection height of emissions. J. Geophys. Res. 112, D10313. doi:10.1029/2006JD008132.

Mao, J., Jacob, D.J., Evans, M.J., et al., 2010. Chemistry of hydrogen oxide radicals ($HO_x$) in the Arctic troposphere in spring. Atmos. Chem. Phys. 10, 5823–5838.

Mieville, A., Granier, C., Liousse, C., Guillaume, B., Mouillot, F., Lamarque, J.-F., Grégoire, J.-M., Pétron, G., 2010. Emissions of gases and particles from biomass burning during the 20th century using satellite data and an historical reconstruction. Atmos. Environ. 44 (11), 1469–1477.

Monks, P.S., Granier, C., Fuzzi, S., et al., 2009. Atmospheric composition change – global and regional air quality. Atmos. Environ. 43 (33), 5268–5350.

Morris, G.A., Hersey, S., Thompson, A.M., et al., 2006. Alaskan and Canadian forest fires exacerbate ozone pollution in Houston, Texas, on 19 and 20 July 2004. J. Geophys. Res. 111, D24S03. doi:10.1029/2006JD007090.

Olson, J.R., Crawford, J.H., Chen, G., et al., 2004. Testing fast photochemical theory during TRACE-P based on measurements of OH, $HO_2$, and $CH_2O$. J. Geophys. Res. 109, D15S10. doi:10.1029/2003JD004278.

Oltmans, S.J., Lefohn, A.S., Harris, J.M., et al., 2010. Enhanced ozone over western North America from biomass burning in Eurasia during April 2008 as seen in surface and profile observations. Atmos. Environ., in press, 44 (35), 4497–4509.

Preston, C.M., Schmidt, M.W.I., 2006. Black (pyrogenic) carbon: a synthesis of current knowledge and uncertainties with special consideration to boreal regions. Biogeosciences 3 (4), 397–420.

Quinn, P.K., Shaw, G., Andrews, E., Dutton, E.G., Ruoho-Airola, T., Gong, S.L., 2007. Arctic haze: current trends and knowledge gaps. Tellus B 59 (1), 99–114.

Quinn, P.K., Bates, T.S., Baum, E., et al., 2008. Short-lived pollutants in the Arctic: their climate impact and possible mitigation strategies. Atmos. Chem. Phys. 8 (6), 1723–1735.

Rahn, K.A., 1981. Relative importances of North America and Eurasia as sources of arctic aerosol. Atmos. Environ. 15 (8), 1447–1455.

Real, E., Law, K.S., Weinzierl, B., et al., 2007. Processes influencing ozone in Alaskan forest fire plumes during long-range transport over the North Atlantic. J. Geophys. Res. 112, D10S41. doi:10.1029/2006JD007576.

Russell, P.B., Bergstrom, R.W., Shinozuka, Y., et al., 2010. Absorption Angstrom Exponent in AERONET and related data as an indicator of aerosol composition. Atmos. Chem. Phys. 10 (3), 1155–1169.

Schultz, M.G., Heil, A., Hoelzemann, J.J., Spessa, A., Thonicke, K., Goldammer, J.G., Held, A.C., Pereira, J.M.C., van het Bolscher, M., 2008. Global wildland fire emissions from 1960 to 2000. Global Biogeochem. Cycles 22, GB2002. doi:10.1029/2007GB003031.

Shaw, G.E., 1995. The Arctic haze phenomenon. Bull. Am. Meteorol. Soc. 76 (12), 2403–2413.

Shindell, D.T., Faluvegi, G., Bauer, S.E., et al., 2007. Climate response to projected changes in short-lived species under an A1B scenario from 2000–2050 in the GISS climate model. J. Geophys. Res. 112, D20103. doi:10.1029/2007JD008753.

Shindell, D.T., Chin, M., Dentener, F., et al., 2008. A multi-model assessment of pollutant transport to the Arctic. Atmos. Chem. Phys. 8 (17), 5353–5372.

Singh, H.B., Salas, L., Herlth, D., et al., 2007. Reactive nitrogen distribution and partitioning in the North American troposphere and lowermost stratosphere. J. Geophys. Res. 112, D12S04. doi:10.1029/2006JD007664.

Singh, H.B., Salas, L.J., Chatfield, R.B., et al., 2004. Analysis of the atmospheric distribution, sources, and sinks of oxygenated volatile organic chemicals (OVOC) based on measurements over the Pacific during TRACE-P. J. Geophys. Res. 109. doi:10.1029/2003JD003883.

Singh, H.B., Salas, L., Herlth, D., et al., 2003. In-situ measurements of HCN and $CH_3CN$ in the Pacific troposphere: sources, sinks, and budgets. J. Geophys. Res. 108 (D20), 8795. doi:10.1029/2002JD003006.

Singh, H.B., Herlth, D., O'Hara, D., et al., 1994. Summertime distribution of PAN and other reactive nitrogen species in the northern high latitude atmosphere of eastern Canada. J. Geophys. Res. 99 (D1), 1821–1835.

Singh, H.B., Herlth, D., O'Hara, D., et al., 1992. Relationship of PAN to active and total odd nitrogen at northern high latitudes: influence of reservoir species on $NO_x$ and $O_3$. J. Geophys. Res. 97 (D15), 16523–16530.

Soja, A.J., Stocks, B., Maczek, P., Fromm, M., Servranckx, R., Turetsky, M., Benscoter, B., 2008. ARCTAS: the perfect smoke. The Canadian Smoke Newsletter, 2–7.

Soja, A.J., Tchebakova, N.M., French, N.H.F., et al., 2007. Climate-induced boreal forest change: predictions versus current observations. Global Planet. Change 56 (3–4), 274–296.

Stocks, B.J., Fosberg, M.A., Lynham, T.J., et al., 1998. Climate change and forest fire potential in Russian and Canadian boreal forests. Clim. Change 38 (1), 1–13.

Stohl, A., 2006. Characteristics of atmospheric transport into the Arctic troposphere. J. Geophys. Res. 111, D11306. doi:10.1029/2005JD006888.

Stone, R.S., Anderson, G.P., Shettle, E.P., et al., 2008. Radiative impact of boreal smoke in the Arctic: observed and modeled. J. Geophys. Res. 113, D14S16. doi:10.1029/2007JD009657.

Stroud, C., Madronich, S., Atlas, E., et al., 2003. Photochemistry in the arctic free troposphere: $NO_x$ budget and the role of odd nitrogen reservoir recycling. Atmos. Environ. 37 (24), 3351–3364.

Van der Werf, G.R., Randerson, J.T., Giglio, L., Collatz, G.J., Kasibhatla, P.S., 2006. Interannual variability in global biomass burning emission from 1997 to 2004. Atmos. Chem. Phys. 6, 3423–3441.

Warneke, C., Bahreini, R., Brioude, J., et al., 2009. Biomass burning in Siberia and Kazakhstan as an important source for haze over the Alaskan Arctic in April 2008. Geophys. Res. Lett. 36, L02813. doi:10.1029/2008GL036194.

Zhang, L., Jacob, D.J., Boersma, K.F., et al., 2008. Transpacific transport of ozone pollution and the effect of recent Asian emission increases on air quality in North America: an integrated analysis using satellite, aircraft, ozonesonde, and surface observations. Atmos. Chem. Phys. 8 (20), 6117–6136.